

pubs.acs.org/JACS Communication

A Spirobifluorene-Based Covalent Organic Framework for Dual Photoredox and Nickel Catalysis

Yingjie Fan, Dong Won Kang, Steven Labalme, and Wenbin Lin*



Cite This: J. Am. Chem. Soc. 2023, 145, 25074–25079



ACCESS I

Metrics & More

Article Recommendations

s Supporting Information

ABSTRACT: Covalent organic frameworks (COFs) have emerged as tunable, crystalline, and porous functional organic materials, but their application in photocatalysis has been limited by rapid excited-state quenching. Herein, we report the first example of dual photoredox/nickel catalysis by an sp² carbon-conjugated spirobifluorene-based COF. Constructed from spirobifluorene and nickel-bipyridine linkers, the NiSCN COF adopted a two-dimensional structure with staggered stacking. Under light irradiation, NiSCN catalyzed amination and etherification/esterification reactions of aryl halides through the photoredox mechanism, with a catalytic efficiency more than 23-fold higher than that of its homogeneous control. NiSCN was used in five consecutive reactions without a significant loss of catalytic activity.

Ovalent organic frameworks (COFs) possess many desirable features such as robust structures, large surface areas, and well-defined pore environments for potential applications in gas separation, conductivity, drug delivery, and catalysis. As interlayer π - π interactions provide an important driving force for COF synthesis, most COFs have two-dimensional (2D) structures with sp² carbon linkages and exhibit rapid exciton diffusion to quench excited states.

We recently reported a photosensitizing 2D pyrene-based COF with long-range π-conjugation and eclipsed stacking of 2D networks.³⁰ This sp² carbon-conjugated COF shows fast energy transfer between pyrene units and Ni-bpy (bpy is 2,2′-bipyridine) moieties to promote the generation of aryl radicals and catalyze photocatalytic borylation and trifluoromethylation of aryl halides, but exhibits low activity in dual photoredox and Ni-catalyzed reactions (e.g., C–O and C–N coupling reactions) due to rapid excited-state quenching and poor redox properties of the pyrene units.³¹ We surmised that less efficient conjugation between the repeating units and staggered stacking between 2D networks would slow excited-state quenching in 2D COFs.^{32,33} Rational incorporation of photosensitizing units and Ni centers in such 2D COFs can facilitate dual photoredox and Ni catalysis (Figure 1).¹⁸

Herein, we report the first example of a 2D COF based on spirobifluorene (**sp**) building blocks for dual photoredox and Ni catalysis. The sterically hindered sp³ carbon-based building blocks not only break the conjugation in 2D networks but also favor staggered stacking to prevent excited-state quenching. The 2D COF with an sp²-carbon linkage, **SCN**, was prepared via Knoevenagel condensation of spirobifluorenyl tetrabenzal-dehyde (**sp**-CHO) and 5,5'-bis(cyanomethyl)-2,2'-bipyridine (bpy-CN) and then coordinated to Ni(II) centers via the bpy moieties to form **NiSCN** (**Figure 2a**). Under light irradiation, the photoexcited **sp** units in **NiSCN** synergized with adjacent Ni(bpy)Br₂ centers to catalyze amination, etherification, and

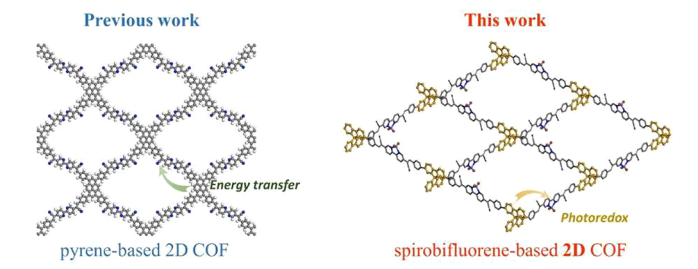


Figure 1. Schematic showing energy transfer catalysis by pyrene-based 2D COF (left)³⁰ and dual photoredox/Ni catalysis by **NiSCN** (right).

esterification of aryl bromides with 23 times higher efficiency than its homogeneous analogs.

Based on the literature precedent of an imine-linked spirobifluorene COF, ^{34,35} we targeted the synthesis of SCN with a C=C linkage from sp-CHO and bpy-CN building blocks. The C=C linkages provide structural rigidity, improved stability, and enhanced energy/electron transfer. ³⁶ Although imine-based COFs have generally shown high crystallinity, only a few sp²-carbon-conjugated COFs with good crystallinity have been reported, due to the poor reversibility of C=C bonds. ^{37,38} Extensive screening of synthetic conditions was carried out (Table S1) and led to the synthesis of SCN through a Knoevenagel reaction between sp-CHO and bpy-CN in 1,4-dioxane with a 4 M aqueous KOH solution at 100 °C (Figure 2a and Table S1). NiSCN was

Received: September 5, 2023 Revised: October 25, 2023 Accepted: November 1, 2023 Published: November 7, 2023





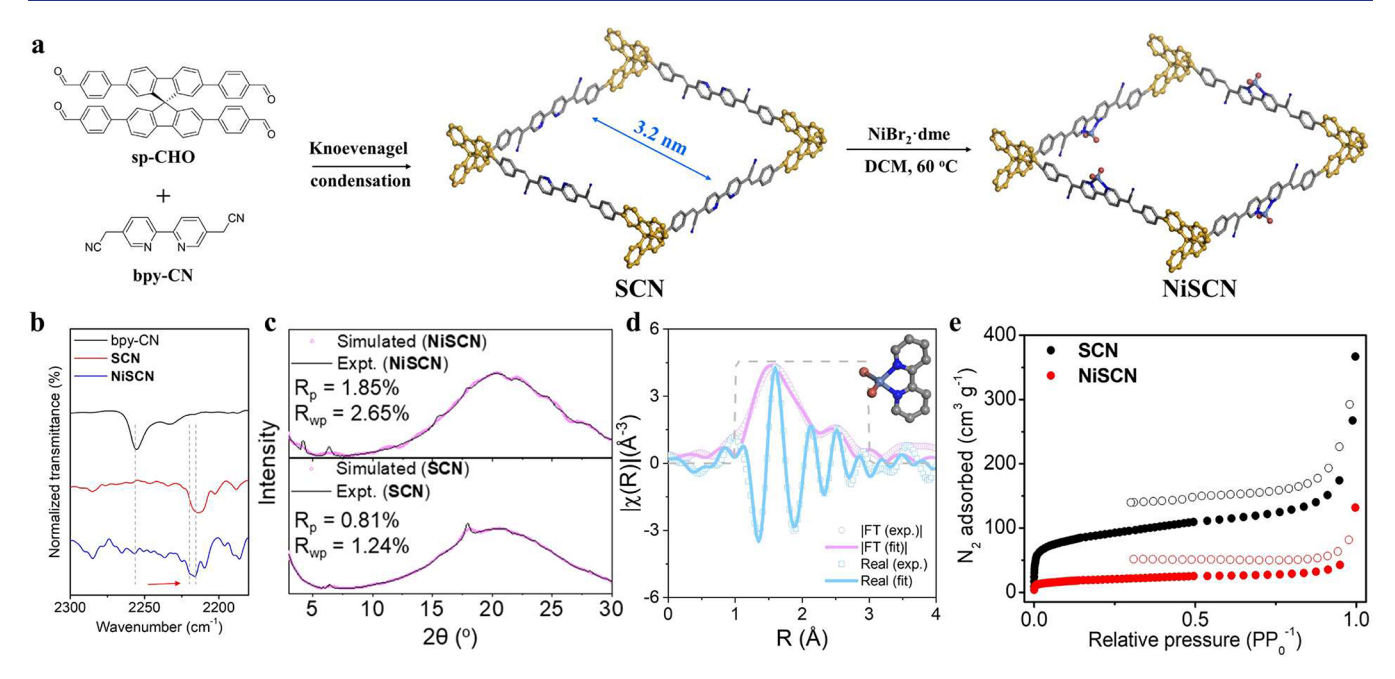


Figure 2. (a) Synthetic scheme of SCN and NiSCN. Gray, C; blue, N; indigo, Ni; red, Br; sp units, yellow. (b) FT-IR spectra of bpy-CN, SCN, and NiSCN in the C≡N stretching region. (c) Simulated and experimental PXRD patterns of SCN and NiSCN. (d) EXAFS analysis of the Ni centers in NiSCN. The structure model of Ni(bpy)Br2 is shown in the inset. (e) Nitrogen sorption isotherms of SCN and NiSCN at 77 K.

obtained by metalation of SCN with NiBr2·dme (dme is ethylene glycol dimethyl ether) in dichloromethane at 60 °C.

After the Knoevenagel condensation, the characteristic C= O stretching vibration of sp-CHO at 1690 cm⁻¹ significantly decreased in intensity in the Fourier transform-infrared (FT-IR) spectrum of SCN (Figure S1). The C=C stretching vibration at 1595 cm⁻¹ increased in intensity due to the formation of the vinyl linkage. The C≡N stretching vibration shifted from 2255 cm⁻¹ in bpy-CN to 2214 cm⁻¹ in SCN and 2216 cm⁻¹ in NiSCN (Figure 2b), indicating π -conjugation between the CN groups and the C=C bonds in SCN and NiSCN.³⁹ The solid-state ¹³C NMR spectrum of SCN showed a new peak at 107.3 ppm for conjugated nitrile groups (Figure S2).

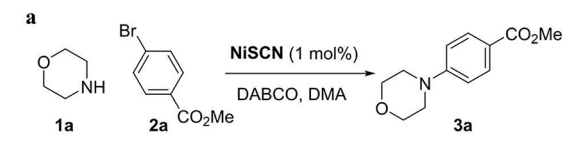
Powder X-ray diffraction (PXRD) studies showed that SCN and NiSCN exhibited 2D network structures with moderate crystallinity. Pawley refinement showed good agreement between the experimental and simulated PXRD patterns of **SCN** with $R_p = 0.81\%$ and $R_{wp} = 1.24\%$. **SCN** adopted staggered stacking of 2D networks due to the nonplanarity of sp units, which disrupts interlayer π – π interaction (Figure 2c and Table S2). Pawley refinement of the experimental PXRD pattern of NiSCN also matched the simulated pattern with R_p = 1.85% and $R_{\rm wp}$ = 2.65%. To our knowledge, **SCN** is the first sp²-carbon conjugated 2D COF with staggered stacking.⁴⁰ The staggered stacking introduced disorder and reduced the crystallinity of SCN.35

X-ray photoelectron spectroscopy (XPS) showed that NiSCN had Ni(II) centers with Ni 2p_{1/2} and 2p_{3/2} peaks at 872.85 and 875.44 eV, respectively (Figure S3). Extended Xray absorption fine structure (EXAFS) analysis showed that the Ni centers in NiSCN adopted a tetrahedral coordination environment similar to that of Ni(bpy)Br₂ with two Ni-N bonds at 1.98 Å and two Ni-Br bonds at 2.35 Å (Figure 2d). N₂ sorption isotherms demonstrated the porosity of SCN and NiSCN with Brunauer-Emmett-Teller surface areas of 322 and 69 m² g⁻¹, respectively (Figure 2e). Density functional

theory calculations gave pore sizes of ~1.5 and ~1.2 nm for SCN and NiSCN, respectively (Figure S4), which matched the expected pore sizes for staggered 2D networks (Figure S4). Transmission electron microscopy imaging showed that SCN and NiSCN exhibited similar spherical morphologies with diameters of 100-200 nm (Figure S5).

Nitrogen-containing compounds are of great significance due to their biological activities. C-N cross-coupling reactions provide a powerful synthetic method to amines. We evaluated NiSCN in dual photoredox and Ni-catalyzed C-N coupling reactions. Under 440 nm irradiation, NiSCN efficiently coupled morpholine (1a) and methyl 4-bromobenzoate (2a) in N,N-dimethylacetamide (DMA) to afford 3a in 91% yield. 41,42 A combination of sp and Ni(dtbbpy)Br₂ produced 3a in 4% yield under identical conditions (Figure 3a, entry 2). Thus, NiSCN outperformed corresponding homogeneous analogues by at least 23 times. Control reactions with SCN and Ni(dtbbpy)Br₂ as the catalyst afforded 3a in 0 and 7% yield, respectively (Figure 3a, entries 3, 4). A combination of SCN and Ni(dtbbpy)Br₂ gave 3a in a 9% yield (Figure 3a, entry 5). A control reaction with NiSCN in the absence of light irradiation did not produce 3a (Figure 3a, entry 6). These results demonstrated the superiority of NiSCN in dual photoredox/Ni-catalyzed amination of 2a over homogeneous controls. In comparison, the reported pyrene-based 2D COF catalyzed the reaction to give 3a in 27% yield (Table S4).30 The majority of 2a was converted to the dehalogenated product (45%).

The C-N coupling reaction can occur via a photoredox process or direct excitation of Ni complexes.^{41,42} Ni complexes were reported to absorb around 425 nm. 42 However, we did not observe product formation with Ni(dtbbpy)Br2 as a catalyst under 440 nm irradiation (Figure 3a entry 5), likely due to the impact of the dtbbpy ligand on the photochemistry of Ni complexes. Based on these results, we propose that the reaction occurs via a photoredox process.



entry	catalyst	yield of 3a (%) ^a
1	NiSCN (1 mol%)	91
2	sp (1 mol%) + NiBr ₂ (dtbbpy) (1 mol%)	4
3	SCN (1 mol%)	0
4	NiBr ₂ (dtbbpy) (1 mol%)	7
5	SCN (1 mol%) + NiBr ₂ (dtbbpy) (1 mol%	5) 9
6 ^b	NiSCN (1 mol%)	0

aNMR yield. bReaction was run in the dark.

b

c

io

Ni(bpy-CN)Br₂

io

-io

-io

-io

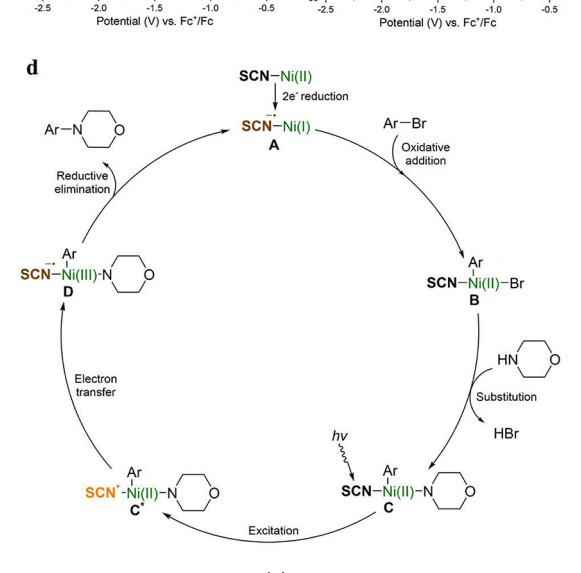


Figure 3. Mechanistic studies. (a) Control experiments for **NiSCN**-catalyzed amination reactions. (b) CV scan of **sp**. (c) CV scan of Ni(bpy-CN)Br₂. (d) Proposed mechanism for **NiSCN**-catalyzed amination reactions.

As cyclic voltammograms (CVs) of COFs typically show broad bands without distinct peaks, we measured the CV of sp and used its redox potential to approximate that of sp units in NiSCN (Figure S11). The CV of sp showed a reversible reduction peak at −1.08 V vs Fc⁺/Fc and irreversible oxidation peaks above 0.5 V (Figures 3b, S11). Emission spectra of NiSCN were measured (Figure S10) to calculate the oxidation potential of excited sp units in the COF according to the thermodynamic cycle. A potential of 1.34 V vs Fc⁺/Fc was calculated as the photo-oxidation potential of sp units in NiSCN. The CV of Ni(bpy-CN)Br₂ showed Ni^{III/II}, Ni^{II/I}, and $Ni^{1/0}$ peaks at 0.62, -0.85, and -1.44 V vs Fc^+/Fc , respectively (Figure 3c, S10). Based on these findings, we propose a mechanistic cycle for NiSCN-catalyzed C-N coupling of aryl bromides under light irradiation (Figures 3d, S13). Because the reduction potential of photoexcited sp only allows the reduction of Ni(II) to Ni(I), the catalytic cycle starts from two-electron reduction of NiSCN by photoexcited sp to

generate Ni(I)-SCN $^{\bullet -}$ (A), a Ni(I) species with a coordinated SCN radical anion. The morpholine substrate serves as a sacrificial reductant in this step. Next, Ar-Br oxidatively adds to Ni(I)-SCN^{o-} to form SCN-Ni(II)(Ar)(Br) (B), which undergoes ligand exchange between Br and morpholine followed by deprotonation of the Ni-coordinated morpholine to form SCN-Ni(II)(Ar)[N(CH₂CH₂)₂O] (C). Photoexcitation initiates electron transfer from Ni(II) to SCN to afford $Ni(III)(Ar)[N(CH_2CH_2)_2O]$ (**D**), which undergoes reductive elimination to yield the product 3a and regenerate the catalyst A. The oxidation power of photoexcited sp units (1.34 V) is higher than the oxidation potential of Ni(II) to Ni(III) (0.62 V). Compared to the previously reported pyrene-based 2D COF,³⁰ the sp units in SCN exhibit a higher oxidation potential in the excited state to promote the reductive elimination step by single-electron transfer. The sp units show the longest absorption at 309 nm in the ultraviolet region, while SCN and NiSCN can both be excited with blue light (Figures S9, S10). The luminescence lifetimes of SCN and NiSCN were determined as 3.26 and 2.31 ns, respectively (Figure S12), which are longer than the reported value for a spirobifluorene analogue (1.56 ns).⁴³ The increased excitedstate lifetime of NiSCN is, in part, responsible for its enhanced photocatalytic efficiency over the homogeneous counterparts.

We next investigated the substrate scope of the NiSCNcatalyzed C-N coupling reactions (Table 1a). Primary and secondary amines were tolerated to yield aniline derivatives 3a, **3b**, **3c**, and **3d** in 91%, 85%, 87%, and 71% yields, respectively. With 10 mol % morpholine as the reductant to access the lowvalent Ni complex, aniline and 4-fluoroaniline were successfully coupled with 2a to give diphenylamines 3e and 3f in 62% and 75% yields. No morpholine-coupled products were observed in these reactions. Electron-deficient aryl bromides with cyano, trifluoromethyl, and acetyl groups underwent coupling reactions to afford aniline 3g, 3h, 3i, and 3j in 92%, 81%, 94%, and 58% yields, respectively. Benzocaine was used in a late-stage functionalization by coupling with 2a to give 3k in a 76% yield (Figure S6). NiSCN was separated from the reaction mixture by filtration and used in five consecutive cycles of coupling reaction between 2a and morpholine (1a) without loss of catalytic activity (Figure S7), demonstrating the stability of NiSCN under the catalytic conditions. Removal of NiSCN by filtration in the sixth run completely stopped the reaction with <1% Ni leaching in the filtrate as determined by ICP-MS. The IR spectrum, PXRD pattern, and XPS spectrum of the recovered NiSCN remained unchanged from those of the pristine NiSCN (Figure S8).

As C—O coupling reactions are also synthetically useful, we tested NiSCN in dual photoredox/Ni-catalyzed C—O coupling reactions. NiSCN efficiently catalyzed the C—O coupling of aryl bromides in *N,N*-dimethylformamide (DMF). Carboxylic acids including acetic acid and benzoic acids were coupled with 2a to afford phenol esters 5a, 5e, and 5f in 65—70% yields. Water and methanol coupled with 2a to afford phenol 5b and anisole 5d in 81% and 84% yield, respectively. Phenol also coupled with 2a to produce diphenyl ether 5c in a 68% yield. Electron-withdrawing groups on the aryl bromides facilitated C—O coupling reactions. Aryl bromides with cyano, ester, and acetyl groups underwent coupling reactions to give 5g, 5h, 5i, and 5j in 78%, 56%, 75%, and 85% yield, respectively. Ibuprofen coupled with 2a to give 5k in 81% yield as an example of late-stage modification (Figure S6). Lastly, NiSCN

Table 1. NiSCN-Catalyzed C-N Coupling and C-O Coupling Reactions of Aryl Bromides

a) C-N coulingb

b) C-O coupling^c

^aIsolated yields. ^b1 (0.3 mmol), 2 (0.2 mmol), DABCO (0.2 mmol), and 2 μ mol of NiSCN in 1 mL of DMA under 440 nm irradiation for 18 h. $^{c}4$ (0.4 mmol), 2 (0.2 mmol), (t-Bu)(i-Pr)NH (0.4 mmol), and 2 μ mol of **NiSCN** in 1 mL of DMF under 440 nm irradiation for 18 h. d0.1 equiv of morpholine was added.

also efficiently catalyzed C-S and C-C coupling reactions as shown in Figure S14.

In summary, we designed a spirobifluorene-based COF for efficient photocatalytic amination and etherification/esterification of aryl bromides via dual photoredox/nickel catalysis. Constructed from spirobifluorene units and Ni-bpy linkers, NiSCN adopted a 2D structure with staggered stacking and reduced excited-state quenching. The photoexcited spirobifluorene units not only efficiently reduced Ni(II) to Ni(I) for oxidative addition of aryl bromide to initiate the catalytic cycle but also oxidized the Ni(II) intermediate to Ni(III) for facile reductive elimination to yield the product and regenerate the catalyst. NiSCN successfully catalyzed C-N coupling and C-O coupling of aryl bromides and exhibited more than 23-fold

higher catalytic efficiency in comparison to its homogeneous control. NiSCN was used in five consecutive reactions without a loss of catalytic activity. This work uncovers a general strategy to construct multifunctional COFs for sustainable synergistic catalysis.

ASSOCIATED CONTENT

Supporting Information

The Supporting Information is available free of charge at https://pubs.acs.org/doi/10.1021/jacs.3c09729.

Materials and methods, synthesis and characterization of COFs, catalytic reactions and characterization of products, control experiments, mechanistic study, NMR spectra (PDF)

AUTHOR INFORMATION

Corresponding Author

Wenbin Lin – Department of Chemistry, The University of Chicago, Chicago, Illinois 60637, United States; orcid.org/0000-0001-7035-7759; Email: wenbinlin@ uchicago.edu

Authors

Yingjie Fan – Department of Chemistry, The University of Chicago, Chicago, Illinois 60637, United States; orcid.org/0000-0003-1857-5788

Dong Won Kang - Department of Chemistry, The University of Chicago, Chicago, Illinois 60637, United States; Department of Chemistry and Chemical Engineering, Inha University, Incheon 22212, Republic of Korea

Steven Labalme - Department of Chemistry, The University of Chicago, Chicago, Illinois 60637, United States

Complete contact information is available at: https://pubs.acs.org/10.1021/jacs.3c09729

Author Contributions

D.W.K. and Y.F. contributed equally.

The authors declare no competing financial interest.

ACKNOWLEDGMENTS

We thank Dr. Alexander Filatov for the help with PXRD measurements and Dr. Justin Jureller for the help with TCSPC measurements. We thank Qijie Shen for helpful discussions. We acknowledge the National Science Foundation (CHE-2102554) and the University of Chicago for funding support and the MRSEC Shared User Facilities at the University of Chicago (DMR-1420709) for instrument access. XAS analysis was performed at Beamline 10-BM, supported by the Materials Research Collaborative Access Team (MRCAT). Use of the Advanced Photon Source, an Office of Science User Facility operated for the U.S. DOE Office of Science by ANL, was supported by the U.S. DOE under Contract DE-AC02-06CH11357.

REFERENCES

(1) Côté, A. P.; Benin, A. I.; Ockwig, N. W.; O'Keeffe, M.; Matzger, A. J.; Yaghi, O. M. Porous, Crystalline, Covalent Organic Frameworks. Science 2005, 310 (5751), 1166-1170.

(2) Li, L.-H.; Feng, X.-L.; Cui, X.-H.; Ma, Y.-X.; Ding, S.-Y.; Wang, W. Salen-Based Covalent Organic Framework. J. Am. Chem. Soc. **2017**, 139 (17), 6042–6045.

- (3) Ma, T.; Kapustin, E. A.; Yin, S. X.; Liang, L.; Zhou, Z.; Niu, J.; Li, L.-H.; Wang, Y.; Su, J.; Li, J.; Wang, X.; Wang, W. D.; Wang, W.; Sun, J.; Yaghi, O. M. Single-crystal x-ray diffraction structures of covalent organic frameworks. *Science* **2018**, *361* (6397), 48–52.
- (4) Diercks, C. S.; Yaghi, O. M. The atom, the molecule, and the covalent organic framework. *Science* **2017**, 355 (6328), No. eaal1585.
- (5) Kandambeth, S.; Mallick, A.; Lukose, B.; Mane, M. V.; Heine, T.; Banerjee, R. Construction of Crystalline 2D Covalent Organic Frameworks with Remarkable Chemical (Acid/Base) Stability via a Combined Reversible and Irreversible Route. *J. Am. Chem. Soc.* 2012, 134 (48), 19524–19527.
- (6) Kang, F.; Wang, X.; Chen, C.; Lee, C.-S.; Han, Y.; Zhang, Q. Construction of Crystalline Nitrone-Linked Covalent Organic Frameworks Via Kröhnke Oxidation. *J. Am. Chem. Soc.* **2023**, *145* (28), 15465–15472.
- (7) Han, X.; Ma, T.; Nannenga, B. L.; Yao, X.; Neumann, S. E.; Kumar, P.; Kwon, J.; Rong, Z.; Wang, K.; Zhang, Y.; Navarro, J. A. R.; Ritchie, R. O.; Cui, Y.; Yaghi, O. M. Molecular weaving of chickenwire covalent organic frameworks. *Chem.* **2023**, *9* (9), 2509–2517.
- (8) Qian, C.; Qi, Q.-Y.; Jiang, G.-F.; Cui, F.-Z.; Tian, Y.; Zhao, X. Toward Covalent Organic Frameworks Bearing Three Different Kinds of Pores: The Strategy for Construction and COF-to-COF Transformation via Heterogeneous Linker Exchange. *J. Am. Chem. Soc.* 2017, 139 (19), 6736–6743.
- (9) Cao, W.; Wang, W. D.; Xu, H.-S.; Sergeyev, I. V.; Struppe, J.; Wang, X.; Mentink-Vigier, F.; Gan, Z.; Xiao, M.-X.; Wang, L.-Y.; Chen, G.-P.; Ding, S.-Y.; Bai, S.; Wang, W. Exploring Applications of Covalent Organic Frameworks: Homogeneous Reticulation of Radicals for Dynamic Nuclear Polarization. *J. Am. Chem. Soc.* **2018**, 140 (22), 6969–6977.
- (10) Guo, J.; Jiang, D. Covalent Organic Frameworks for Heterogeneous Catalysis: Principle, Current Status, and Challenges. ACS Cent. Sci. 2020, 6 (6), 869–879.
- (11) Kang, D. W.; Kang, M.; Yun, H.; Park, H.; Hong, C. S. Emerging Porous Solid Electrolytes for Hydroxide Ion Transport. *Adv. Funct. Mater.* **2021**, *31* (19), 2100083.
- (12) Kim, J. H.; Kang, D. W.; Yun, H.; Kang, M.; Singh, N.; Kim, J. S.; Hong, C. S. Post-synthetic modifications in porous organic polymers for biomedical and related applications. *Chem. Soc. Rev.* **2022**, *51* (1), 43–56.
- (13) Han, B.; Jin, Y.; Chen, B.; Zhou, W.; Yu, B.; Wei, C.; Wang, H.; Wang, K.; Chen, Y.; Chen, B.; Jiang, J. Maximizing Electroactive Sites in a Three-Dimensional Covalent Organic Framework for Significantly Improved Carbon Dioxide Reduction Electrocatalysis. *Angew. Chem., Int. Ed.* **2022**, *61* (1), No. e202114244.
- (14) Chen, Z.; Wang, K.; Tang, Y.; Li, L.; Hu, X.; Han, M.; Guo, Z.; Zhan, H.; Chen, B. Reticular Synthesis of One-Dimensional Covalent Organic Frameworks with 4-c sql Topology for Enhanced Fluorescence Emission. *Angew. Chem., Int. Ed.* **2023**, 62 (1), No. e202213268.
- (15) Kan, X.; Wang, J.-C.; Chen, Z.; Du, J.-Q.; Kan, J.-L.; Li, W.-Y.; Dong, Y.-B. Synthesis of Metal-Free Chiral Covalent Organic Framework for Visible-Light-Mediated Enantioselective Photooxidation in Water. *J. Am. Chem. Soc.* **2022**, *144* (15), 6681–6686.
- (16) Han, X.; Huang, J.; Yuan, C.; Liu, Y.; Cui, Y. Chiral 3D Covalent Organic Frameworks for High Performance Liquid Chromatographic Enantioseparation. *J. Am. Chem. Soc.* **2018**, *140* (3), 892–895.
- (17) Sun, T.; Xie, J.; Guo, W.; Li, D.-S.; Zhang, Q. Covalent-Organic Frameworks: Advanced Organic Electrode Materials for Rechargeable Batteries. *Adv. Energy Mater.* **2020**, *10* (19), 1904199.
- (18) Jati, A.; Dey, K.; Nurhuda, M.; Addicoat, M. A.; Banerjee, R.; Maji, B. Dual Metalation in a Two-Dimensional Covalent Organic Framework for Photocatalytic C-N Cross-Coupling Reactions. *J. Am. Chem. Soc.* **2022**, *144* (17), 7822–7833.
- (19) Lin, W.; Lin, J.; Zhang, X.; Zhang, L.; Borse, R. A.; Wang, Y. Decoupled Artificial Photosynthesis via a Catalysis-Redox Coupled COF||BiVO4 Photoelectrochemical Device. *J. Am. Chem. Soc.* **2023**, 145 (32), 18141–18147.

- (20) Duan, H.; Li, K.; Xie, M.; Chen, J.-M.; Zhou, H.-G.; Wu, X.; Ning, G.-H.; Cooper, A. I.; Li, D. Scalable Synthesis of Ultrathin Polyimide Covalent Organic Framework Nanosheets for High-Performance Lithium-Sulfur Batteries. *J. Am. Chem. Soc.* **2021**, *143* (46), 19446–19453.
- (21) Jati, A.; Dam, S.; Kumar, S.; Kumar, K.; Maji, B. A π -conjugated covalent organic framework enables interlocked nickel/photoredox catalysis for light-harvesting cross-coupling reactions. *Chem. Sci.* **2023**, 14 (32), 8624–8634.
- (22) Nguyen, V.; Grünwald, M. Microscopic Origins of Poor Crystallinity in the Synthesis of Covalent Organic Framework COF-5. *J. Am. Chem. Soc.* **2018**, *140* (9), 3306–3311.
- (23) Xu, S.; Richter, M.; Feng, X. Vinylene-Linked Two-Dimensional Covalent Organic Frameworks: Synthesis and Functions. *Acc. Mater. Res.* **2021**, 2 (4), 252–265.
- (24) Chandra, S.; Kandambeth, S.; Biswal, B. P.; Lukose, B.; Kunjir, S. M.; Chaudhary, M.; Babarao, R.; Heine, T.; Banerjee, R. Chemically Stable Multilayered Covalent Organic Nanosheets from Covalent Organic Frameworks via Mechanical Delamination. *J. Am. Chem. Soc.* **2013**, *135* (47), 17853–17861.
- (25) Waller, P. J.; Gándara, F.; Yaghi, O. M. Chemistry of Covalent Organic Frameworks. Acc. Chem. Res. 2015, 48 (12), 3053–3063.
- (26) Meng, Y.; Luo, Y.; Shi, J. L.; Ding, H.; Lang, X.; Chen, W.; Zheng, A.; Sun, J.; Wang, C. 2D and 3D Porphyrinic Covalent Organic Frameworks: The Influence of Dimensionality on Functionality. *Angew. Chem., Int. Ed.* **2020**, *59* (9), 3624–3629.
- (27) Wang, G.-B.; Wang, Y.-J.; Kan, J.-L.; Xie, K.-H.; Xu, H.-P.; Zhao, F.; Wang, M.-C.; Geng, Y.; Dong, Y.-B. Construction of Covalent Organic Frameworks via a Visible-Light-Activated Photocatalytic Multicomponent Reaction. *J. Am. Chem. Soc.* **2023**, *145* (9), 4951–4956.
- (28) Zhang, X.; Geng, K.; Jiang, D.; Scholes, G. D. Exciton Diffusion and Annihilation in an sp2 Carbon-Conjugated Covalent Organic Framework. *J. Am. Chem. Soc.* **2022**, *144* (36), 16423–16432.
- (29) Yuan, C.; Fu, S.; Yang, K.; Hou, B.; Liu, Y.; Jiang, J.; Cui, Y. Crystalline C—C and C=C Bond-Linked Chiral Covalent Organic Frameworks. *J. Am. Chem. Soc.* **2021**, *143* (1), 369–381.
- (30) Fan, Y.; Kang, D. W.; Labalme, S.; Li, J.; Lin, W. Enhanced Energy Transfer in A π -Conjugated Covalent Organic Framework Facilitates Excited-State Nickel Catalysis. *Angew. Chem., Int. Ed.* **2023**, 62 (11), No. e202218908.
- (31) Romero, N. A.; Nicewicz, D. A. Organic Photoredox Catalysis. *Chem. Rev.* **2016**, *116* (17), 10075–10166.
- (32) Lin, G.; Ding, H.; Yuan, D.; Wang, B.; Wang, C. A Pyrene-Based, Fluorescent Three-Dimensional Covalent Organic Framework. *J. Am. Chem. Soc.* **2016**, *138* (10), 3302–3305.
- (33) Yang, M.; Hanayama, H.; Fang, L.; Addicoat, M. A.; Guo, Y.; Graf, R.; Harano, K.; Kikkawa, J.; Jin, E.; Narita, A.; Müllen, K. Saturated Linkers in Two-Dimensional Covalent Organic Frameworks Boost Their Luminescence. *J. Am. Chem. Soc.* **2023**, *145* (26), 14417–14426.
- (34) Liu, Y. Y.; Li, X. C.; Wang, S.; Cheng, T.; Yang, H.; Liu, C.; Gong, Y.; Lai, W. Y.; Huang, W. Self-templated synthesis of uniform hollow spheres based on highly conjugated three-dimensional covalent organic frameworks. *Nat. Commun.* **2020**, *11* (1), 5561.
- (35) Zhao, J.; Xie, M.; Chen, X.; Jin, J.-K.; Zhao, W.; Luo, J.; Ning, G.-H.; Liu, J.; Li, D. A BODIPY-Based 1D Covalent Organic Framework for Photocatalytic Aerobic Oxidation. *Chem.—Asian J.* **2023**, *18* (13), No. e202300328.
- (36) He, T.; Geng, K.; Jiang, D. All sp2 carbon covalent organic frameworks. *Trends Chem.* **2021**, 3 (6), 431–444.
- (37) Li, X. sp2carbon-conjugated covalent organic frameworks: synthesis, properties, and applications. *Mater. Chem. Front.* **2021**, 5 (7), 2931–2949.
- (38) Xu, S.; Richter, M.; Feng, X. Vinylene-Linked Two-Dimensional Covalent Organic Frameworks: Synthesis and Functions. *Acc. Mater. Res.* **2021**, 2 (4), 252–265.
- (39) Bu, R.; Zhang, L.; Liu, X. Y.; Yang, S. L.; Li, G.; Gao, E. Q. Synthesis and Acid-Responsive Properties of a Highly Porous

- Vinylene-Linked Covalent Organic Framework. ACS Appl. Mater. Interfaces 2021, 13 (22), 26431–26440.
- (40) Wang, S.; Li, X. X.; Da, L.; Wang, Y.; Xiang, Z.; Wang, W.; Zhang, Y. B.; Cao, D. A Three-Dimensional sp(2) Carbon-Conjugated Covalent Organic Framework. *J. Am. Chem. Soc.* **2021**, 143 (38), 15562–15566.
- (41) Corcoran, E. B.; Pirnot, M. T.; Lin, S.; Dreher, S. D.; DiRocco, D. A.; Davies, I. W.; Buchwald, S. L.; MacMillan, D. W. C. Aryl amination using ligand-free Ni(II) salts and photoredox catalysis. *Science* **2016**, 353 (6296), 279–283.
- (42) Lim, C.-H.; Kudisch, M.; Liu, B.; Miyake, G. M. C-N Cross-Coupling via Photoexcitation of Nickel-Amine Complexes. *J. Am. Chem. Soc.* **2018**, 140 (24), 7667–7673.
- (43) Thiery, S.; Tondelier, D.; Declairieux, C.; Geffroy, B.; Jeannin, O.; Métivier, R.; Rault-Berthelot, J.; Poriel, C. 4-Pyridyl-9,9'-spirobifluorenes as Host Materials for Green and Sky-Blue Phosphorescent OLEDs. *J. Phys. Chem. C* **2015**, *119* (11), 5790–5805.